Received: 18 July 2021 | Revised: 8 September 2021 | Accepted: 11 October 2021

DOI: 10.1002/ese3.1001

ORIGINAL ARTICLE

Energy Science & Engineering Open Access

Impacts of De-NO_x system layouts of a diesel passenger car on exhaust emission factors and monetary penalty

Jianbing Gao[1,2] | **Haibo Chen**[2] | **Ye Liu**[2] | **Ying Li**[3]

[1]School of Mechnical Engineering, Beijing Institute of Technology, Beijing, China

[2]Institute for Transport Studies, University of Leeds, Leeds, UK

[3]Dynnoteq, Kington, UK

Correspondence
Jianbing Gao, School of Mechnical Engineering, Beijing Institute of Technology, Beijing 100081, China; Institute for Transport Studies, University of Leeds, Leeds LS2 9JT, UK.
Email: redonggaojianbing@163.com

Funding information
Horizon 2020 Framework Programme, Grant/Award Number: 815189

Abstract

Automobile emissions are significantly dependent on the after-treatment system performance, which is partly determined by exhaust temperature. Regarding diesel passenger cars, after-treatment systems generally include diesel oxidation catalyst (DOC), diesel particulate filter (DPF), and selective catalytic reduction (SCR). The layouts affect their temperature variations because of the heat loss and thermal capacity of tailpipes and after-treatment systems. As for the original layout of DOC+DPF+SCR, nitrogen oxides (NO_x) emissions are the main concerns of diesel vehicle emissions, especially under cold-start conditions. Ammonia Creation and Conversion Technology (ACCT) system shows excellent performance of reducing cold-start NO_x emissions; additionally, the damage costs of individual exhaust emissions are different greatly, which may change the priority of emission reductions when considering monetary penalty. In this article, the impacts of the after-treatment system layouts on the exhaust emission reductions were investigated based on a diesel passenger car; additionally, SCR and ACCT systems as the De-NO_x devices were adopted individually in corresponding scenarios; the after-treatment system layouts were assessed from the viewpoints of both emission factors and monetary penalty. The results indicated that the ACCT system presented much better NO_x reduction effectiveness than SCR system over different layouts. NO_x reduction efficiency was very sensitive to vehicle operation conditions over the upstream layouts of NO_x reduction devices. The layout-1 of DOC+ACCT+DPF showed the lowest global emission factors from the diesel passenger car. DPF was much easier to achieve regeneration under the original layout conditions due to its shortest distance to the engine. The layout-2 of ACCT+DOC+DPF had the minimum monetary penalty factor of exhaust emissions from this diesel passenger car.

KEYWORDS

after-treatment system layout, ammonia creation and conversion technology, damage costs, diesel passenger cars, emission factors, selective catalytic reduction

1 | INTRODUCTION

With the increase of the amounts of automobiles, the problems caused by exhaust emissions are becoming more and more prominent.[1-3] As indicated by the report,[4] carbon dioxide (CO_2) emission from transportations account for 29% of the total CO_2 emission, being the largest proportion, followed by electricity, industry. Nitrogen oxides (NO_x), particulate matter ($PM_{2.5}$), and volatile organic compounds (VOCs) from automobiles contribute to large proportions of total hazardous emissions, being approximately 35%, 5%, and 20%, respectively, indicated by Minnesota Pollution Control Agency.[5] Emission regulations aiming to drop automobile emissions are becoming more and more stringent[6]; additionally, real driving emissions (RDE) test procedure is also introduced.[7] Compared with standard driving cycles such as Worldwide harmonized Light vehicles Test Cycles (WLTC),[8] the real driving conditions are more complicated and variable, which leads to higher emission factors over real driving than WLTC.[9,10] The issue of higher RDE than laboratory emissions is mainly for CO_2 of all vehicles and NO_x of diesel vehicles. It was demonstrated that Euro 6b diesel cars emitted emit 5-16 times of NO_x in the real world than certification tests[11]; meantime, CO_2 emission was 1.4-1.8 times of the certificated values. CO_2 emission of a Euro 6 gasoline passenger car was approximately 194 g/km under real-world driving conditions, being much higher than that of standard driving cycles (lower than 100 g/km).[12] Previous studies addressed the importance of reducing real-world CO_2 and NO_x emissions. Yang et al[13] also demonstrated that NO_x and CO_2 emissions were critical to address RDE of Euro 6 passenger cars.

With regard to the current techniques mitigating automobile emissions, the effective measures aim to increase after-treatment efficiency[14-16] and decrease emission formations by controlling in-cylinder combustion.[17-19] As for the current mature technologies, in-cylinder control usually brings about fuel penalty, although it can drop emissions to a low level. In order to meet stricter emission regulations, after-treatment systems are indispensable to balance the emission formations and fuel consumptions. One of the most important factors correlating the after-treatment system efficiency is temperature.[20] The effectiveness of catalyst-based after-treatment systems is excellent under high exhaust temperature conditions where the emission reduction efficiency can be higher than 90%.[21,22] However, their performance under cold-start conditions is poor.[23] According to Gao et al's study,[24] exhaust emissions during engine warm-up process accounted more than 50% of the total emissions over the given trips. Heeb et al[25] demonstrated that approximately 70% of the total carbon monoxide (CO) emission over Federal Test Procedure (FTP) (1400 s in total) was caused by the first 500 s of the trip. Research[26] compared exhaust emission rates of different vehicles, demonstrating that the emission rates over cold start were much higher than hot start, with the maximum difference being higher than 100 times of hot-start emissions. Additionally, the emissions were significantly worsened by low ambient temperature for passenger cars meeting different emission regulations due to much heat loss by tailpipe and upstream after-treatment systems.[27] It was consistent with the conclusions of the reference[28] which addressed unregulated emissions as well. Du et al[29] researched the RDE under cold-start conditions, revealing that the cold-start period accounted for a significant proportion of the total urban driving emissions; meantime, the cold-start emissions were very sensitive to driving behaviors; additionally, the correlations between cold-start emissions and ambient temperature were addressed. The impacts of cold-start emissions by driving behaviors were also discussed in Gao et al's study.[30] Many technologies are investigated to drop cold-start emissions such as burners,[31] reformers,[32] thermal insulations,[33,34] heat storage materials,[35] electric catalytic converters (eHC),[36] Ammonia Creation and Conversion Technology (ACCT),[37] Ammonia Storage and Delivery systems (ASDS)[38]; meantime, some of these measures are helpful for diesel particulate filter (DPF) regeneration. The main purposes of these technologies are to increase exhaust temperature or provide an easier way to supply reactants (eg, gaseous ammonia), ensuring high efficiency of after-treatment systems. Gao et al[30] discussed their effectiveness, energy penalty, and complexity. Regarding the common layouts of after-treatment systems (DOC+DPF+SCR), NO_x emissions are the main concerns. ACCT system as a new technique aiming to drop cold-start NO_x emissions has excellent performance and no energy penalty.[37] It used exhaust energy to hydrolyze AdBlue into gaseous CO_2, water (H_2O), and ammonia (NH_3) under high exhaust temperature conditions; then, they were formed as a new product (ACCT fluid) after cooling down. ACCT fluid was much easier than AdBlue to provide gaseous NH_3 under relative low-temperature conditions.

One of the vital factors affecting SCR efficiency was the exhaust temperature,[39,40] which is related to the engine operation conditions and the distance of the SCR system to the engine. For the after-treatment systems being the downstream of others, there was a temperature drop and lag caused by heat loss and thermal capacity of the tailpipes and upstream after-treatment systems.[41,42] Lao et al[43] investigated the impacts of after-treatment system layouts on diesel engine emissions. It indicated that DOC+DPF+SCR layout was found to be more beneficial than DOC+SCR+DPF under specific conditions. DPF-in-front system was more robust regarding the changes in emission regulations. Gurupatham et al[44] also researched the effect of after-treatment layouts on the global performance of DOC, DPF, and SCR. Moving SCR to the downstream of DPF led to the drop of NO_x reduction under cold-start conditions; however, it was benefited for DPF regeneration. He et al[45] simulated the after-treatment system performance over various layouts, with the results indicating that the individual after-treatment systems had correlative impacts on their emission reduction efficiency.

In fact, the reductions of some individual emissions from vehicles should have priorities determined by social, human health, and economic impacts, which are considered in the damage costs. The damage cost of NO_x emissions was much higher than CO and hydrocarbon (HC)[46]; additionally, SCR system was placed the downstream of DOC and DPF systems for the common layouts. It caused much NO_x emissions from cold start and warm-up process. When considering the emission reductions from the perspective of monetary penalty, SCR system should have a higher priority than DOC in after-treatment layouts. DPF efficiency depended less on the exhaust temperature, but the regeneration has the requirements of high temperature. Taken the monetary penalty into consideration, the optimal layouts of the after-treatment systems would be different.

According to the government report,[46] the damage cost of the individual air pollutants is different. Regarding the regular exhaust emissions from internal combustion engine vehicles, particulate matter (PM) has the highest damage cost, followed by NO_x and HC[46]; the damage cost of PM is thousands times higher than HC; additionally, the damage cost of CO is much lower than others.[47] The applications of monetary penalty factors calculated from emission factors and corresponding damage cost can be used to assess the impacts from vehicle exhausts. To the authors' knowledge, this is the first time to estimate the monetary penalty factors of exhaust emissions from passenger cars over various after-treatment layouts. In this study, emission characteristics of a diesel passenger car were investigated using a numerical simulation method when the diesel passenger car was equipped with different De-NO_x devices; the effectiveness of the after-treatment systems were discussed under various layout conditions; meantime, the monetary penalty factors of the exhaust emissions were used to assess their overall impacts on environment, human health, and society, which provides a new insight to regulate the exhaust emissions.

2 | MATERIALS AND METHODS

In this section, the simulation models were described in detail, the vehicle model and ACCT model were validated using experimental data, and various layouts of after-treatment systems were provided.

TABLE 1 Specifications of the diesel passenger car, reproduced from Gao et al[60]

Specifications	Value
Vehicle mass	1505 kg
Maximum speed	170 km·h^{-1}
Gear number	6
Fuel	Diesel
Engine type	In-line, four cylinder, four stroke
Intake type	Turbocharged intercooler
Fuel injection type	Direct injection
Engine max power/kW	103 kW @ 4000 rpm
Engine max torque/N·m	325 N·m @ 1500 rpm
Stroke/mm	80.4
Bore/mm	79.1
Compression ratio	16.5
Emission regulation	Euro 6
Original after-treatment	DOC+DPF+SCR
Mileage/km	853

2.1 | Simulation model description

A vehicle simulation model was set up using GT-SUITE software, including a powertrain model, an after-treatment system submodel, and an emission submodel.

2.1.1 | Descriptions of the vehicle model

The vehicle used in this investigation was a Euro 6 compliant diesel passenger car whose power source was a four-cylinder, four-stroke, turbocharged diesel engine. The specifications of the diesel vehicle are shown in Table 1. The maximum power output of the diesel vehicle was 103 kW, corresponding to the engine speed of 4000 rpm. The compression ratio of the diesel engine was 16.5. The simulation model of the diesel passenger car is shown in Figure 1. This vehicle model included three modules, which were vehicle powertrains, emission sources, and after-treatment systems. Engine model, transmission model, and control model were included in the powertrain system; the engine model was based on experimental tests, including brake-specific fuel consumption and brake mean effective pressure maps. In order to consider the effect of cold start on pipe-out emissions, the maps of exhaust temperature, emission factors, and exhaust flow rates were included in the emission model. With regard

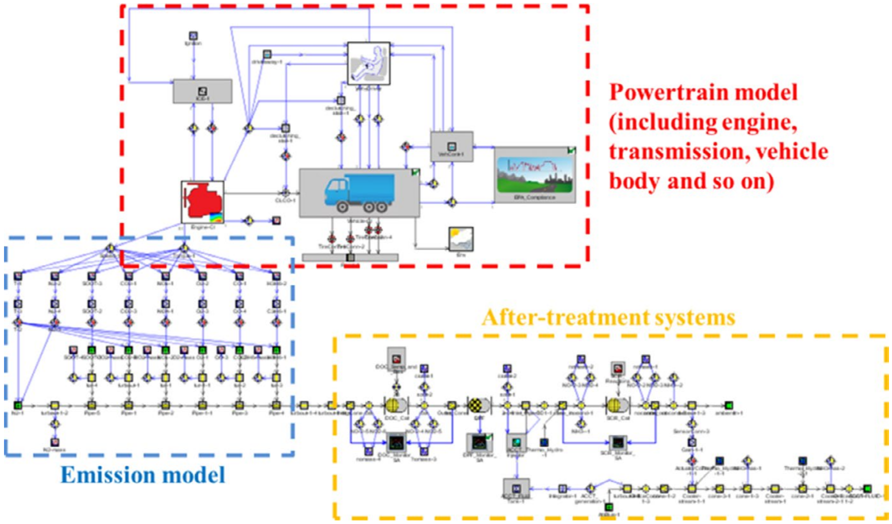

FIGURE 1 Simulation model of the diesel passenger car, reproduced from the work of Gao et al[30]

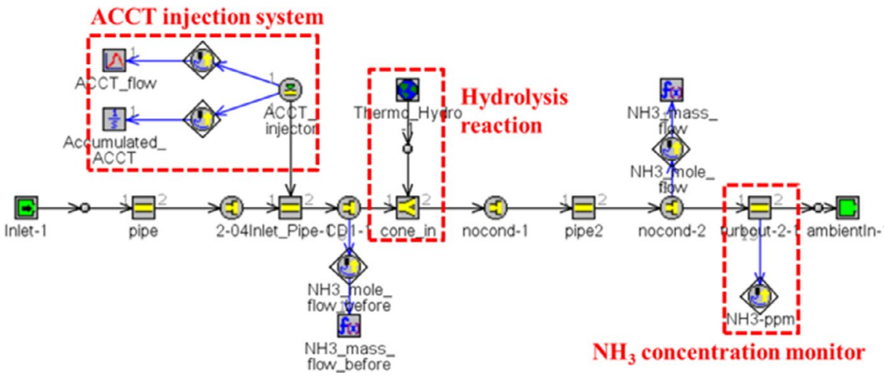

FIGURE 2 Simulation model of ACCT fluid hydrolysis reactions, reproduced from the work of Gao et al[30]

to the after-treatment system, it included a DOC, a DPF, and a SCR. The DOC was followed by a DPF, being at the upstream of a SCR device.

2.1.2 | Descriptions of after-treatment systems

The main concerns on the gaseous exhaust emissions from diesel passenger cars were NO_x. In order to meet stricter emission regulations, for example, Euro 7, the SCR system could be replaced by an ACCT system to further decrease NO_x emissions by effectively delivering gaseous ammonia under low exhaust temperature conditions. The operation theory of the ACCT system was reported in the reference.[37] The ACCT system was consist of an AdBlue tank, an AdBlue pump, an ACCT reactor, an ACCT fluid tank, and an ACCT fluid injector (see Figure 2). AdBlue was injected into the ACCT rector under high exhaust temperature conditions; then, AdBlue was hydrolyzed into CO_2, gaseous water, and gaseous ammonia under the assistance of exhaust energy; furthermore, the gaseous hydrolyzed products were cooled down in the ACCT tank, being converted into ACCT fluid (a new product). The hydrolysis temperature of ACCT fluid was much lower than AdBlue such that ACCT fluid was more effective to drop NO_x emissions under low exhaust temperature conditions, such as urban driving, stop-and-go scenarios.

2.1.3 | Descriptions of the after-treatment system layouts

Layouts of the after-treatment systems affected the emission reduction efficiency, DPF regeneration, and the energy penalty. The scenarios of the after-treatment system layouts in this investigation are shown in Figure 3. Due to high effectiveness of ACCT system dropping NO_x emissions, it may generate impacts on the layouts of after-treatment systems in terms of optimal global performance. In this investigation, three different after-treatment layouts were provided. The changes of after-treatment layouts inevitably affected after-treatment efficiency due to the temperature changes accordingly; additionally, it would influence DPF regeneration processes, which required high exhaust temperature. Regarding the DPF regeneration, passive regeneration using nitrogen dioxide (NO_2) or catalyst was adopted in the work; and the difference

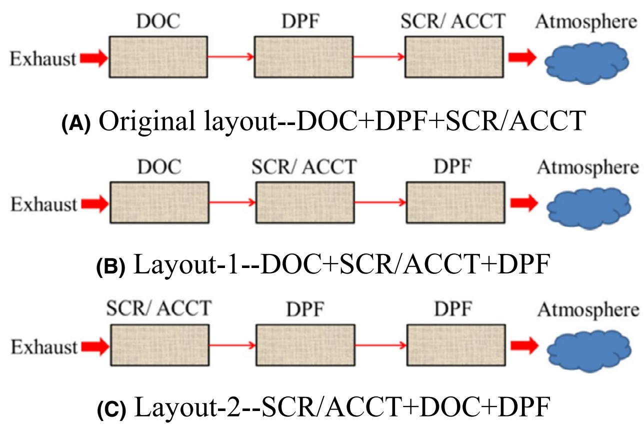

FIGURE 3 Scenarios of the after-treatment system layouts

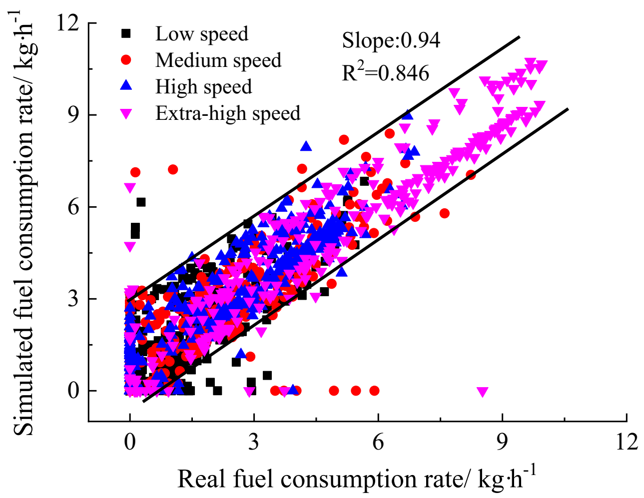

FIGURE 4 Validations of the vehicle fuel consumption, reproduced from the work of Gao et al[60]

of DPF regeneration over various after-treatment layouts was explored.

2.2 | Validations of simulation models

In order to estimate the vehicle emissions with high precisions, the vehicle model including the fuel consumption and exhaust emissions over original after-treatment layout was validated using experimental tests.

2.2.1 | Validations of vehicle model

Validations of the vehicle model using fuel consumption were based on WLTC, as shown in Figure 4. Simulation results over high vehicle speed matched better with the test results than low vehicle speed conditions. Over low vehicle speed conditions, the fuel consumption rates were low such that small errors would cause a significant difference between simulation and test results. Only small amounts of simulated results showed notable deviations with the test results. Figure 5 compares NO_x emission rates of experimental and simulation results for both engine-out and pipe-out emissions. The difference between experimental and simulation results was minor, which indicated high precisions of the emission models and SCR model (including the chemical reactions). Concluded from Figures 4 and 5, the vehicle simulation model was accurate to do the future research. As shown in Figure 5, NO_x formation was the highest over high-speed and extra-high-speed regimes. NO_x formation rates under low-speed conditions were quite low due to low in-cylinder combustion temperature. However, the pipe-out emission rates were almost zero over high-speed and extra-high-speed regimes, benefiting from high NO_x reduction efficiency. At the start of the driving cycle, the exhaust temperature was low, leading to low SCR efficiency. The main focus of the current enhanced NO_x reduction techniques was cold-start regimes.

2.2.2 | Validations of ACCT system

ACCT system was validated using experimental tests separately. The boundary conditions of the ACCT simulation model were the same as the ones in the work described previously.[37] The boundary conditions of the simulation and test were: hot air flow rates, 250 kg/h; ACCT fluid flow rates, 400 g/h; air temperature at 100°C, 150°C, 200°C, 300°C, and 400°C; ammonia (NH_3) monitoring point, 800 mm downstream of the ACCT fluid injector. Each scenario lasted 30 s in the experiment.[37] Comparisons of simulation and test results are shown in Figure 6. As indicated in the work of Wilson et al,[37] ACCT fluid was almost fully hydrolyzed over 100°C; however, the tested NH_3 concentration was slightly lower than the simulation results, which was caused by NH_3 films forming on the walls of the pipes used in the test. If the test lasted longer, NH_3 concentration would approach 500 ppm after the NH_3 absorption by the pipe walls was saturated. The precision of the ACCT simulation model was acceptable for the future investigation.

3 | RESULTS AND DISCUSSION

In this section, exhaust emissions and monetary penalty factors over different after-treatment system layouts and DPF regeneration strategies were explored; additionally, the De-NO_x measures including the normally used SCR technique and the ACCT system were adopted in

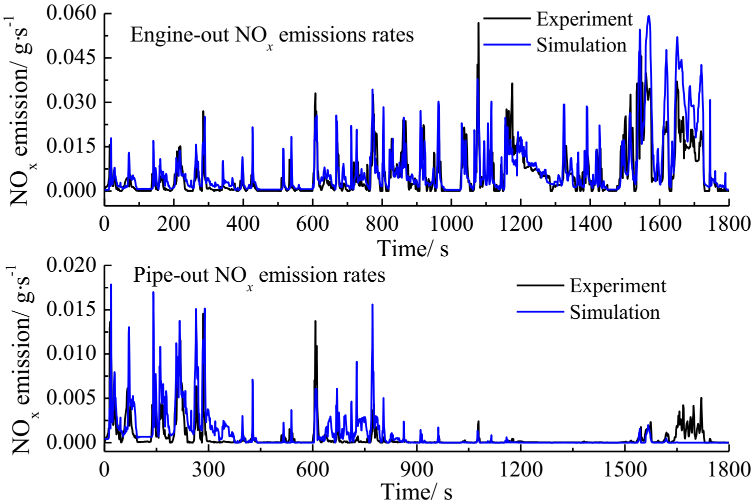

FIGURE 5 Validations of vehicle exhaust emissions over original after-treatment layout, reproduced from the work of Gao et al[30]

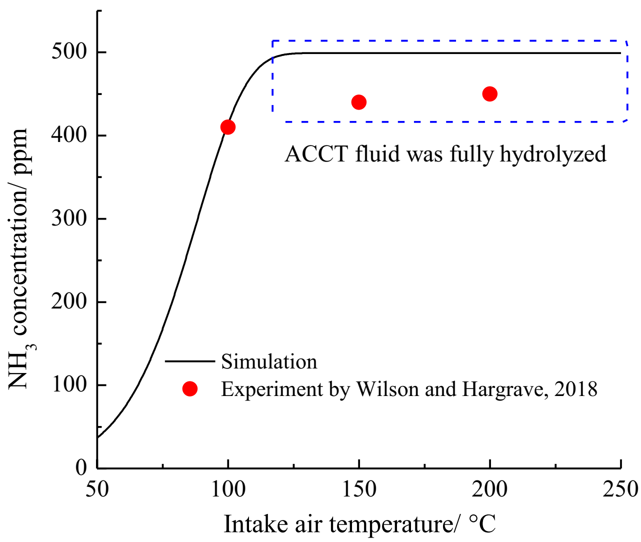

FIGURE 6 Validations of ACCT fluid hydrolysis reactions, reproduced from the work of Gao et al[30]

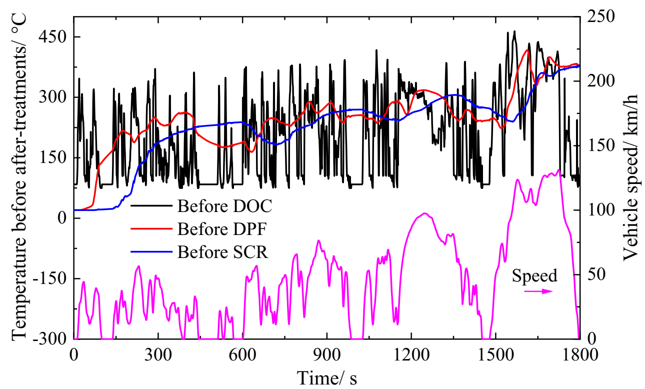

FIGURE 7 Exhaust temperature before individual after-treatment systems

individual scenarios. Monetary penalty factors were calculated using exhaust emission factors and damage cost.

3.1 | Exhaust emissions over different after-treatment system layouts

In this section, exhaust emissions including CO, HC, NO_x, and PM over various after-treatment layouts were reported when the diesel passenger car was equipped with different De-NO_x systems, namely SCR and ACCT systems.

3.1.1 | Exhaust emissions over various layouts

Efficiency of the DOC, SCR, ACCT, and DPF regeneration were significantly dependent on the exhaust temperature, which would be affected by vehicle operation conditions, thermal capacity, and heat loss by tailpipes and upstream after-treatment systems. The exhaust temperature at different positions of the pipeline is shown in Figure 7. The temperature presented in this figure was corresponding to the original layout of after-treatment systems. As can be seen, the exhaust temperature before DOC changed significantly with vehicle operation conditions, and it had a similar pattern with vehicle speed. High vehicle speed usually led to high exhaust temperature, although the temperature was more relied on vehicle accelerations. At the start of the cycle, the after-treatment temperature was low, leading to the formation of N_2O emission in SCR. According to Yang et al's study,[48] the exhaust temperature before after-treatment systems presented high dependency on the vehicle speed under real driving conditions. The temperature before DPF was much smoother than that before DOC due to heat loss and thermal capacity of upstream systems. Because of the large volume of DOC and its thermal capacity, there was a temperature lag before DPF. Thermal capacity of the DOC device could alleviate the temperature changes caused by the heating and cooling effect. The temperature profile before SCR device had a similar pattern with that before DPF, but it had an approximately 100-s delay. According to the reference,[20] the exhaust temperature of SCR system was much smoother than the patterns of vehicle speed, which agreed with the authors' results. It was also supported by the results[49] under real driving conditions where smooth temperature profiles were observed after after-treatment systems. As for this diesel passenger car over WLTC, it took more than 200 s for the temperature before SCR to reach the light-off value. Regarding a heavy duty diesel vehicle under real driving conditions, the warm-up durations lasted more than 1000 s where the temperature before SCR was lower than 100°C.[50] There were lots of vehicle stop events where the temperature dropped significantly due to the idling. In the real-world tests, the temperature distributions changed significantly with vehicle driving situations.[50] Over most of the operation time, the engine was under low engine load conditions.

Distributions of NO_x emission rates over different after-treatment system layouts for SCR scenarios are shown in Figure 8. Proportions of high NO_x emission rates dropped significantly regardless of the after-treatment system layouts. Layout-2 had the highest proportions of low NO_x emission rates, followed by layout-1 due to their shorter distance to the engine than the original layout. The proportions of NO_x emission rates being higher than 0.01 g/s were nearly zero for layout-1 and layout-2. Distributions of CO and HC emissions over various scenarios when the vehicle was equipped with SCR/ACCT are presented in Figures S1 and S2. Since SCR and ACCT systems only affected NO_x emissions, CO distributions over SCR and ACCT scenarios were almost the same. The proportion of engine-out CO emission rates being smaller than 0.004 g/s was quite low; and the proportion decreased generally with the increase of emission rates when CO emission rates were higher than 0.004 g/s. Regarding pipe-out CO emission rates, the distributions over the original layout were the same as layout-1 because the DOC position was the same. The CO emission rates were mainly focused on the values being lower than 0.002 g/s. Compared with original layout and layout-1, the proportion of high CO emission rates increased slightly for layout-2. Under the impacts of after-treatment system layouts, the HC distribution patterns were similar to CO.

For different after-treatment system layouts, the difference in pipe-out NO_x emission rates was mainly caused by SCR efficiency, which is shown in Figure 9. It was obvious that SCR efficiency was low at the start of the driving cycle, especially for original layout and layout-1. SCR efficiency of layout-1 had a similar pattern with original layout, which was consistent with the temperature evolutions (Figure 7). Because SCR system was the closest to the engine for layout-2, the temperature was higher than the other two layouts at the first 150 s, resulting in higher SCR efficiency. SCR efficiency was almost 100% for the three different layouts after 900 s. The efficiency was dropped significantly for layout-1 around 600 s and original layout around 700 s due to the temperature decrease in those periods, which was caused by low vehicle speed around 550 s. Figure S3 shows the proportions of CO reductions by DOC over various after-treatment system layouts. CO reductions reached nearly 100% in a short time after vehicle started for original layout and layout-1; however, it took more than 200 s for layout-2 to achieve high CO reduction efficiency. HC presented a similar pattern (see Figure S4), but the fluctuations of HC reduction efficiency were higher than CO. According to

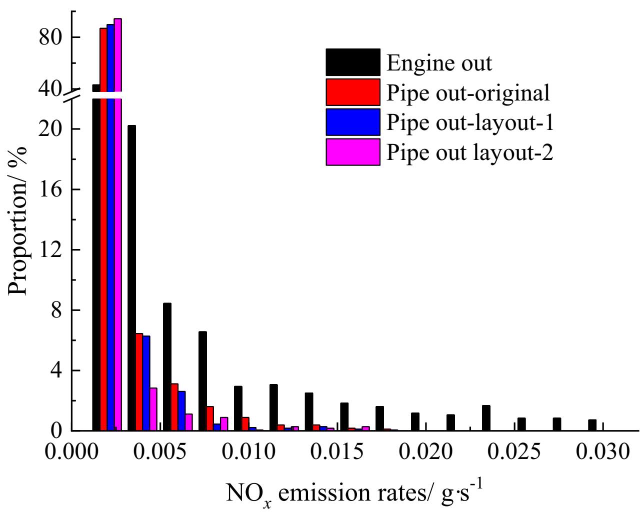

FIGURE 8 Distributions of NO_x emission rates of various scenarios over SCR adoptions

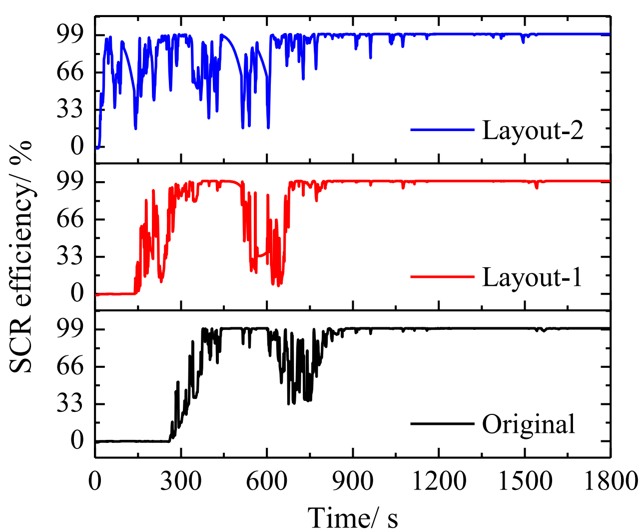

FIGURE 9 SCR efficiency over various layouts

Boriboonsomsin et al,[50] the time-average NO_x reductions by SCR were lower than 80% for majorities of the vehicle groups. Exhaust emissions were also sensitive to ambient temperature, especially for NO_x emissions which were increased from approximately 0.09 g/km to 0.67 g/km over WLTC when the ambient temperature was decreased from 23°C to −5°C.[51] Lower ambient temperature meant more heat loss. The temperatures used in Ko et al's study[51] were in the common ranges for many countries. It implied that the emissions would be worse in winter.

Due to lower light-off temperature of ACCT system than SCR system, NO_x emission rates over ACCT scenarios were lower than corresponding SCR scenarios. Proportions of NO_x emission rates being higher than 0.0075 g/s were quite low, as shown in Figure 10; NO_x emission rates were mainly focused on the regions being lower than 0.005 g/s. Figure 11 shows the ACCT efficiency of NO_x reductions over various after-treatment system layouts. Compared with SCR scenarios, the low-efficiency regions were much less for ACCT scenarios. The "zero-flat" durations for the original layout and layout-1 were shorter than corresponding SCR scenarios. Regarding layout-1, the efficiency drop around 680 s was weakened by comparing with SCR scenarios, and the efficiency drop around 750 s was limited for original layout. Such excellent performance of ACCT system was also demonstrated by Gao et al's study.[30] The comparisons of the average ACCT and SCR efficiency over different after-treatment layout are shown in Table 2. The efficiency improvement of the SCR and ACCT efficiency by the layout were significant; meantime, the efficiency improvement by enhanced De-NO_x system was the highest over the original layout among the three scenarios.

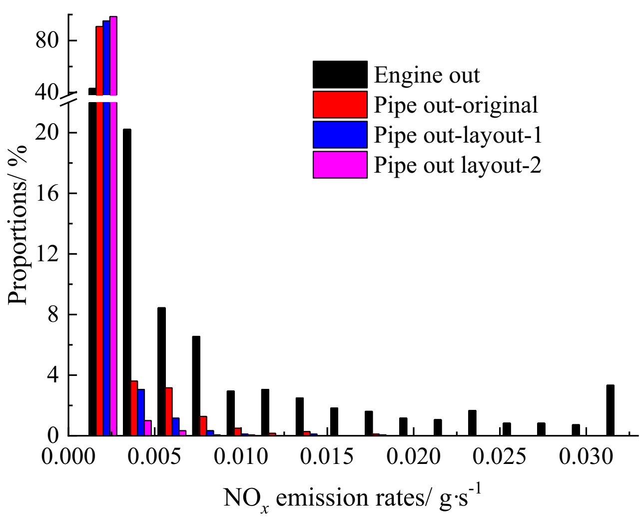

FIGURE 10 Distributions of NO_x emission rates of various scenarios over ACCT adoptions

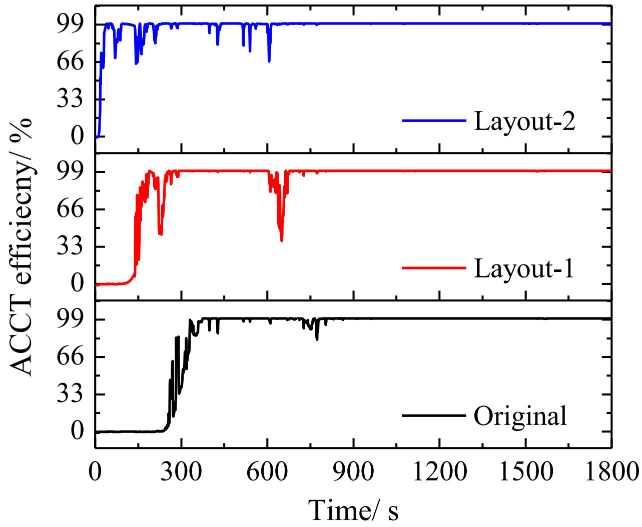

FIGURE 11 ACCT efficiency over various layouts

TABLE 2 Average efficiency of SCR and ACCT system

	NO_x reduction efficiency/ %		
	Original layout	**Layout-1**	**Layout-2**
SCR	77.5	81.9	89.5
ACCT	83.3	90.1	97.8

3.2 | DPF regeneration over different after-treatment layouts

Different from DOC and SCR/ACCT systems whose efficiency was significantly dependent on the exhaust temperature, DPF efficiency was mainly relied on the designs and the engine operation conditions (PM concentration and exhaust flow rates). DPF regeneration process was dependent on the exhaust temperature. Figure 12 shows DPF efficiency over NO_x assistant regeneration scenarios. Under relative low-temperature conditions, chemical reactions between NO_x and DPF could occur,[52] which achieve the continuous regeneration of DPF. DPF efficiency was almost the same over different layouts in the first 1100 s; the difference between the original layout and layout-1/layout2 was slightly enlarged in 1100 s-1800 s. It was mainly caused by the DPF regeneration process. As indicated by Meng et al,[53,54] the particle number and average particle diameter increased during the DPF regeneration process. It was also consistent with Bensaid et al's opinion.[55] Under the NO_x assistant regeneration conditions, it could avoid much PM depositions. The difference of DPF efficiency between NO_x assistant regeneration and catalyst assistant regeneration was limited over individual after-treatment layouts (see Figures S5 and S6).

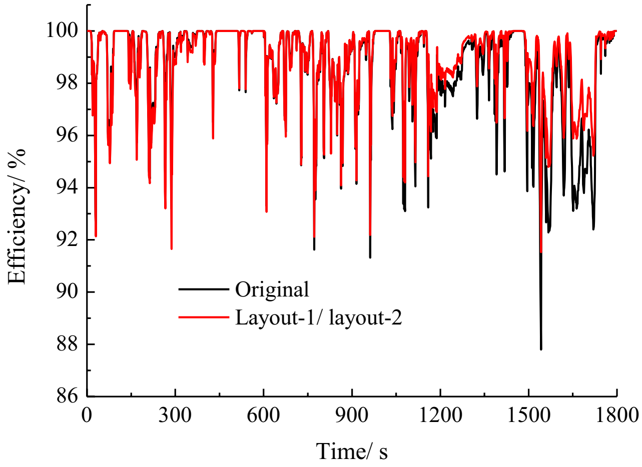

FIGURE 12 DPF efficiency over NO_x assistant regeneration scenarios for both SCR and ACCT scenarios

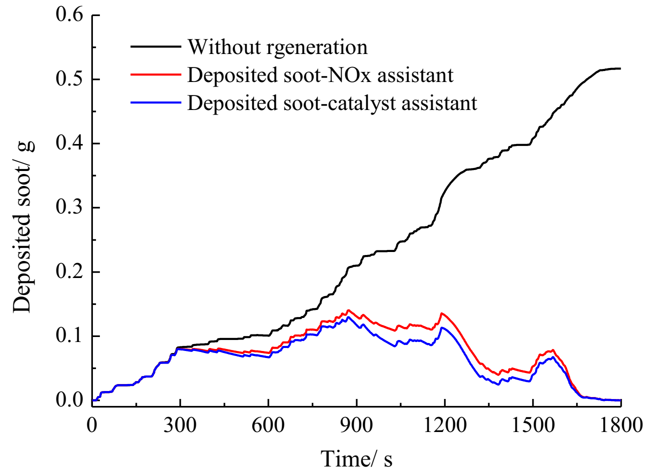

FIGURE 13 DPF regeneration over original layout

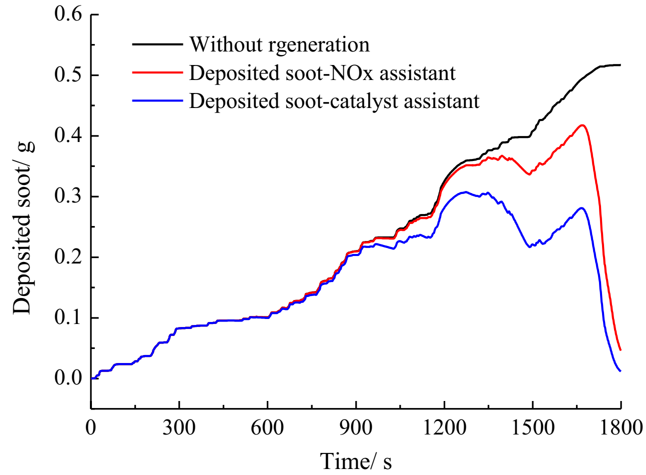

FIGURE 14 DPF regeneration over layout-1/layout-2

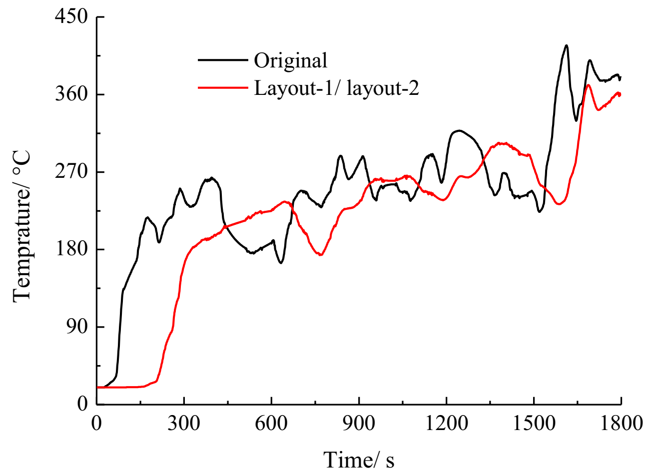

FIGURE 15 Temperature before DPF

Regeneration process of DPF system could be reflected by the amount of soot depositions on filters, as shown in Figures 13 and 14. As can be seen, the amounts of soot depositions increased continuously if without any regeneration measures, which could led to the significant increase of the engine backpressure.[56] The regeneration process started from around 300 s for the original layouts; however, it was around 1000 s for the other two layouts. When the exhaust temperature was higher than 200°C, the soot oxidation rates increased significantly.[52] By analyzing the test data from Jiao et al and Rossomando et al,[52,57] DPF regeneration temperature over catalyst scenarios was higher than NO_x scenarios; however, the catalyst assistant regeneration was slightly easier than NO_x assistant regeneration for all the after-treatment layouts in this study. Due to the existing of NO_x in exhaust, the catalyst assistant regeneration also included the impacts from NO_x assistant regeneration in theory. Regarding the original layout, the temperature before DPF was higher than the other two layouts (see Figure 15) because the DPF was closer to the engine. As for the DPF regeneration, DOC+DPF closed couple strategy was more efficient.

3.3 | Exhaust emission factors and monetary penalty factors

Exhaust emission factors over WLTC were investigated under various after-treatment system layouts, and results are shown in Tables 3 and 4. As can be seen from the tables, the exhaust emission factors were lower than the limitations of Euro 6 emission regulation for both SCR and ACCT scenarios. Without considering the DPF regeneration problems such as energy needed, layout-1 and layout-2 presented better performance than the original layout regarding emission factors, which was caused

TABLE 3 Exhaust emission factors when the vehicle was equipped with a SCR system

	$CO/g{\cdot}km^{-1}$	$HC/g{\cdot}km^{-1}$	$NO_x/g{\cdot}km^{-1}$	$PM/mg{\cdot}km^{-1}$	
				NO_x R	Catalyst-R
Original layout	0.012	0.007	0.069	0.897	0.909
Layout-1	0.012	0.007	0.047	0.802	0.841
Layout-2	0.024	0.023	0.034	0.802	0.841

Abbreviation: R, regeneration.

TABLE 4 Exhaust emission factors when the vehicle was equipped with an ACCT system

	$CO/g{\cdot}km^{-1}$	$HC/g{\cdot}km^{-1}$	$NO_x/g{\cdot}km^{-1}$	$PM/mg{\cdot}km^{-1}$	
				NO_x-R	Catalyst-R
Original layout	0.012	0.007	0.046	0.897	0.909
Layout-1	0.012	0.007	0.023	0.802	0.841
Layout-2	0.024	0.024	0.008	0.802	0.841

Abbreviation: R, regeneration.

by the improved overall thermal status of after-treatment systems. Layout-2 showed the lowest NO_x emission factor, although the CO emission factor was doubled. It should be noted that PM emission factors over NO_x assistant regeneration scenarios were slightly lower than catalyst assistant regeneration. Compared with layout-1 and layout-2, the original layout presented the highest PM emission factors due to insufficient NO_x emissions (in DPF) which conduced to oxidizing PM. Due to lower hydrolysis temperature of ACCT fluid, NO_x emissions factors over ACCT system were much lower than SCR scenarios. SCR system and ACCT system presented limited impacts on PM emission factors. It was indicated in the reference,[20] SCR efficiency reached the maximum value under the exhaust temperature of 350°C, and the efficiency dropped gradually with increasing temperature. Additionally, the optimal exhaust temperature for SCR efficiency changed with the types of catalyst coating on SCR.[50] Regarding the upstream layouts for SCR system, the exhaust temperature was lower than 400°C over WLTC; however, exhaust temperature could be much higher when the vehicle operated at high load conditions, such as operating under the uphill conditions for a long period in real driving conditions. SCR system should be avoided the closest distance to the engine. Under the real driving test, average NO_x emission factors for Euro 6 compliant diesel vehicles was approximately 0.31 $g{\cdot}km^{-1}$ in urban areas; the value was around 0.2 $g{\cdot}km^{-1}$ for motorway.[58] The RDE was much higher than WLTC results; additionally, the emission factors over urban driving were higher than motorway. It addressed the importance of high efficient after-treatment systems and the challenge of lowering NO_x emissions under low-speed conditions. As for the real-world driving,[59] low vehicle speed conditions had the highest emission factors, especially for NO_x emissions. Based on the authors' previous investigation,[14] eHC technique was used to decrease the exhaust emissions during cold-start conditions. The effectiveness of eHC was higher than ACCT system; however, eHC brought about much energy penalty which was inconsistent with the low-carbon driving requirements.

Due to the differences in damage cost of the individual exhaust pollutants, the monetary penalty factors of exhaust emissions would be much different from exhaust emission factors, as shown in Tables 5 and 6. The damage cost of individual exhaust emissions from government report is shown in Table S1. Due to high damage cost of NO_x and PM emissions, the monetary penalty factors of NO_x and PM emissions were much higher than CO and HC emissions for both SCR and ACCT scenarios. Original layout presented the highest monetary penalty factor, and layout-2 had the lowest factor, regarding both individual and total monetary penalty factors. The factors under ACCT scenarios were much lower than SCR scenarios. DPF regeneration approach showed minor impacts on total monetary penalty factors. NO_x emission should have the priority in order to drop the monetary penalty factors, followed by PM because of their high proportions in total factors.

4 | CONCLUSIONS

In order to investigate the impacts of after-treatment system layouts on exhaust emissions and corresponding monetary penalty factors, a diesel passenger car was simulated over WLTC; additionally, the effect of De-NO_x systems (SCR and ACCT systems) on the exhaust emissions and monetary penalty factors were discussed. The main conclusions are as follows:

TABLE 5 Monetary penalty factors of exhaust emissions when the vehicle was equipped with a SCR system

	$CO/\times10^{-4}$ $P\cdot(km)^{-1}$	$HC/\times10^{-4}$ $P\cdot(km)^{-1}$	$NO_x/\times10^{-2}$ $P\cdot(km)^{-1}$	$PM/\times10^{-3}$ $P\cdot(km)^{-1}$		$Total/\times10^{-2}$ $P\cdot(km)^{-1}$	
				NO_x-R	Catalyst-R	NO_x-R	Catalyst-R
Original layout	1.22	7.14	4.41	6.58	6.67	5.08	5.09
Layout-1	1.22	7.14	3.00	5.89	6.17	3.61	3.64
Layout-2	2.45	2.35	2.17	5.89	6.17	2.81	2.84

Abbreviations: P, penny; R, regeneration.

TABLE 6 Monetary penalty factors of exhaust emissions when the vehicle was equipped with an ACCT system

	$CO/\times10^{-4}$ $P\cdot(km)^{-1}$	$HC/\times10^{-4}$ $P\cdot(km)^{-1}$	$NO_x/\times10^{-2}$ $P\cdot(km)^{-1}$	$PM/\times10^{-3}$ $P\cdot(km)^{-1}$		$Total/\times10^{-2}$ $P\cdot(km)^{-1}$	
				NO_2-R	Catalyst-R	NO_x-R	Catalyst-R
Original layout	1.22	7.14	2.94	6.58	6.67	3.61	3.62
Layout-1	1.22	7.14	1.47	5.89	6.17	2.08	2.11
Layout-2	2.45	2.45	0.51	5.89	6.17	1.15	1.18

Abbreviations: P, penny; R, regeneration.

1. After-treatment temperature was sensitive to the vehicle speed when it was close to the engine; the longer the distance of the after-treatment systems to the engine, the smoother and lower the temperature profile was. For SCR and ACCT scenarios, NO_x emission distributions presented similar patterns over various layouts; however, ACCT scenarios showed a lower proportion over high emission rate regions.
2. ACCT scenarios presented higher NO_x reduction efficiency than SCR scenarios under different layout conditions, especially the first 800 s of WLTC NO_x reduction efficiency over original layout and layout-1 showed similar patterns, but there was a lag of approximately 130 s for the original layout. As for the DPF regeneration, original layout was much easier than layout-1 and layout-2, caused by higher DPF temperature.
3. ACCT system showed lower NO_x emission factors and monetary penalty factors than SCR system over the three different layouts. Regarding the emission factors meeting the limits of emission regulations, layout-1 presented the best performance; however, layout-2 was the best from the viewpoints of dropping monetary penalty factors.

ACKNOWLEDGMENT

The research reported in this article was jointly supported by the EU-funded project MODALES (grant agreement no. 815189).

ORCID

Jianbing Gao https://orcid.org/0000-0002-9724-5789

REFERENCES

1. Wu Y, Zhang S, Hao J, et al. On-road vehicle emissions and their control in China: a review and outlook. *Sci Total Environ*. 2017;574:332-349.
2. Reşitoğlu İA, Altinişik K, Keskin A. The pollutant emissions from diesel-engine vehicles and exhaust aftertreatment systems. *Clean Technol Environ Policy*. 2015;17:15-27.
3. Gao J, Wang X, Song P, Tian G, Ma C. Review of the backfire occurrences and control strategies for port hydrogen injection internal combustion engines. *Fuel*. 2022;307: 121553.
4. EPA. *Sources of Greenhouse Gas Emissions*. EPA; 2020.
5. Agency MPC. *Sources of Air Pollution that Most Impact Health*. Agency MPC; 2020.
6. Awad OI, Ma X, Kamil M, Ali OM, Zhang Z, Shuai S. Particulate emissions from gasoline direct injection engines: a review of how current emission regulations are being met by automobile manufacturers. *Sci Total Environ*. 2020;718: 137302.
7. Hooftman N, Messagie M, Van Mierlo J, Coosemans T. A review of the European passenger car regulations – Real driving emissions vs local air quality. *Renew Sustain Energy Rev*. 2018;86:1-21.
8. Tutuianu M, Bonnel P, Ciuffo B, et al. Development of the World-wide harmonized Light duty Test Cycle (WLTC) and a possible pathway for its introduction in the European legislation. *Transp Res Part D: Transp Environ*. 2015;40:61-75.
9. García-Contreras R, Soriano JA, Fernández-Yáñez P, et al. Impact of regulated pollutant emissions of Euro 6d-Temp light-duty diesel vehicles under real driving conditions. *J Clean Prod*. 2020;286:124927.
10. Valverde V, Mora BA, Clairotte M, et al. Emission factors derived from 13 Euro 6b light-duty vehicles based on laboratory and on-road measurements. *Atmosphere*. 2019;10:243.
11. Triantafyllopoulos G, Dimaratos A, Ntziachristos L, Bernard Y, Dornoff J, Samaras Z. A study on the CO_2 and NO_x emissions performance of Euro 6 diesel vehicles under various chassis

dynamometer and on-road conditions including latest regulatory provisions. *Sci Total Environ*. 2019;666:337-346.
12. Dimaratos A, Toumasatos Z, Doulgeris S, Triantafyllopoulos G, Kontses A, Samaras Z. Assessment of CO_2 and NO_x emissions of one diesel and one bi-fuel gasoline/CNG Euro 6 vehicles during real-world driving and laboratory testing. *Front Mech Eng*. 2019;5:62.
13. Yang Z, Liu Y, Wu L, et al. Real-world gaseous emission characteristics of Euro 6b light-duty gasoline-and diesel-fueled vehicles. *Transp Res Part D: Transp Environ*. 2020;78: 102215.
14. Gao J, Tian G, Sorniotti A. On the emission reduction through the application of an electrically heated catalyst to a diesel vehicle. *Energy Sci Eng*. 2019;7:2383-2397.
15. Dey S, Dhal GC, Mohan D, Prasad R. Application of hopcalite catalyst for controlling carbon monoxide emission at cold-start emission conditions. *J Traffic Transp Eng (English Edition)*. 2019;6:419-440.
16. Gumus M. Reducing cold-start emission from internal combustion engines by means of thermal energy storage system. *Appl Therm Eng*. 2009;29:652-660.
17. Gong C, Li J, Peng L, et al. Numerical investigation of intake oxygen enrichment effects on radicals, combustion and unregulated emissions during cold start in a DISI methanol engine. *Fuel*. 2019;253:1406-1413.
18. Calam A, Aydoğan B, Halis S. The comparison of combustion, engine performance and emission characteristics of ethanol, methanol, fusel oil, butanol, isopropanol and naphtha with n-heptane blends on HCCI engine. *Fuel*. 2020;266: 117071.
19. Labecki L, Ganippa L. Effects of injection parameters and EGR on combustion and emission characteristics of rapeseed oil and its blends in diesel engines. *Fuel*. 2012;98:15-28.
20. Wang X, Song G, Wu Y, Yu L, Zhai Z. A NO_x Emission model incorporating temperature for heavy-duty diesel vehicles with urea-SCR systems based on field operating modes. *Atmosphere*. 2019;10:337.
21. Luján JM, Climent H, García-Cuevas LM, Moratal A. Pollutant emissions and diesel oxidation catalyst performance at low ambient temperatures in transient load conditions. *Appl Therm Eng*. 2018;129:1527-1537.
22. Misra C, Ruehl C, Collins J, Chernich D, Herner J. In-use NO_x emissions from diesel and liquefied natural gas refuse trucks equipped with SCR and TWC, respectively. *Environ Sci Technol*. 2017;51:6981-6989.
23. Zare A, Nabi MN, Bodisco TA, et al. Diesel engine emissions with oxygenated fuels: a comparative study into cold-start and hot-start operation. *J Clean Prod*. 2017;162:997-1008.
24. Gao J, Tian G, Sorniotti A, Karci AE, Di Palo R. Review of thermal management of catalytic converters to decrease engine emissions during cold start and warm up. *Appl Therm Eng*. 2019;147:177-187.
25. Heeb N, Forss A, Wilhelm P. Comparison of methane, benzene and alkyl benzenes cold start emission data of EURO I and EURO II three-way catalyst passenger cars and light duty vehicles from time resolved exhaust gas analysis. *Proceedings of the 10th International Symposium Transport and Air Pollution*; 2001, p. 93.
26. Ko J, Son J, Myung C-L, Park S. Comparative study on low ambient temperature regulated/unregulated emissions characteristics of idling light-duty diesel vehicles at cold start and hot restart. *Fuel*. 2018;233:620-631.
27. Weilenmann M, Favez J-Y, Alvarez R. Cold-start emissions of modern passenger cars at different low ambient temperatures and their evolution over vehicle legislation categories. *Atmos Environ*. 2009;43:2419-2429.
28. Weilenmann M, Soltic P, Saxer C, Forss A-M, Heeb N. Regulated and nonregulated diesel and gasoline cold start emissions at different temperatures. *Atmos Environ*. 2005;39:2433-2441.
29. Du B, Zhang L, Geng Y, Zhang Y, Xu H, Xiang G. Testing and evaluation of cold-start emissions in a real driving emissions test. *Transp Res Part D: Transp Environ*. 2020;86: 102447.
30. Gao J, Chen H, Liu Y, et al. The effect of after-treatment techniques on the correlations between driving behaviours and NO_x emissions of a passenger cars. *J Clean Prod*. 2021;288: 125647.
31. Akcayol MA, Cinar C. Artificial neural network based modeling of heated catalytic converter performance. *Appl Therm Eng*. 2005;25:2341-2350.
32. Kirwan JE, Quader AA, Grieve MJ. Fast start-up on-board gasoline reformer for near zero emissions in spark-ignition engines. SAE Technical Paper. 2002.
33. Burch SD, Potter TF, Keyser MA, Brady MJ, Michaels KF. Reducing cold-start emissions by catalytic converter thermal management. *SAE Transac*. 1995;348-353.
34. Daya R, Singh MR, Hoard J, Chanda S. Insulated catalyst with heat storage for real world vehicle emissions reduction. ASME 2016 Internal Combustion Engine Division Fall Technical Conference: American Society of Mechanical Engineers, 2016, p. V001T04A6-VT04A6.
35. Gumus M, Ugurlu A. Application of phase change materials to pre-heating of evaporator and pressure regulator of a gaseous sequential injection system. *Appl Energy*. 2011;88:4803-4810.
36. Pace L, Presti M. An alternative way to reduce fuel consumption during cold start: the electrically heated catalyst. SAE Technical Paper. 2011.
37. Wilson JG, Hargrave G. Analysis of a novel method for low-temperature ammonia production using DEF for mobile selective catalytic reduction systems. SAE Technical Paper. 2018.
38. Johannessen T, Schmidt H, Svagin J, Johansen J, Oechsle J, Bradley R. Ammonia storage and delivery systems for automotive NO_x aftertreatment. SAE Technical Paper. 2008.
39. García A, Monsalve-Serrano J, Villalta D, Sari RL. Performance of a conventional diesel aftertreatment system used in a medium-duty multi-cylinder dual-mode dual-fuel engine. *Energy Convers Manage*. 2019;184:327-337.
40. Lafossas F, Matsuda Y, Mohammadi A, et al. Calibration and validation of a diesel oxidation catalyst model: from synthetic gas testing to driving cycle applications. *SAE Int J Engines*. 2011;4:1586-1606.
41. Qiu T, Li X, Liang H, Liu X, Lei Y. A method for estimating the temperature downstream of the SCR (selective catalytic reduction) catalyst in diesel engines. *Energy*. 2014;68:311-317.
42. El-Sharkawy A, Sami A, Hekal AE-R, Arora D, Khandaker M. Transient modelling of vehicle exhaust surface temperature. *SAE Int J Mater Manuf*. 2016;9:321-329.
43. Lao CT, Akroyd J, Eaves N, et al. Investigation of the impact of the configuration of exhaust after-treatment system for diesel engines. *Appl Energy*. 2020;267: 114844.
44. Gurupatham A, He Y. Architecture design and analysis of diesel engine exhaust aftertreatment system and comparative study

with close-coupled DOC-DPF System. *SAE Int J Fuels Lubr*. 2009;1:1387-1396.
45. He N, Jiang Z, Ning Z. Comparison of catalytic conversion characteristics of different integrated aftertreatment systems in diesel engine. *J Phys: Conference Series: IOP Publishing*. 2020;1578. 012218.
46. UK Government. *Air Quality Appraisal: Damage Cost Guidance*. In: Affairs DfEFR, ed. London: The UK government; 2020.
47. Wang MQ, Santini DJ. *Estimation of Monetary Values of Air Pollutant Emissions in Various US Areas*. Argonne National Lab.; 1994.
48. Yang Z, Ge Y, Thomas D, et al. Real driving particle number (PN) emissions from China-6 compliant PFI and GDI hybrid electrical vehicles. *Atmos Energy*. 2019;199:70-79.
49. Ko J, Myung C-L, Park S. Impacts of ambient temperature, DPF regeneration, and traffic congestion on NO_x emissions from a Euro 6-compliant diesel vehicle equipped with an LNT under real-world driving conditions. *Atmos Energy*. 2019;200:1-14.
50. Boriboonsomsin K, Durbin T, Scora G, et al. Real-world exhaust temperature profiles of on-road heavy-duty diesel vehicles equipped with selective catalytic reduction. *Sci Total Environ*. 2018;634:909-921.
51. Ko J, Jin D, Jang W, Myung C-L, Kwon S, Park S. Comparative investigation of NO_x emission characteristics from a Euro 6-compliant diesel passenger car over the NEDC and WLTC at various ambient temperatures. *Appl Energy*. 2017;187:652-662.
52. Jiao P, Li Z, Shen B, Zhang W, Kong X, Jiang R. Research of DPF regeneration with NO_x-PM coupled chemical reaction. *Appl Therm Eng*. 2017;110:737-745.
53. Meng Z, Chen C, Li J, et al. Particle emission characteristics of DPF regeneration from DPF regeneration bench and diesel engine bench measurements. *Fuel*. 2020;262: 116589.
54. Meng Z, Li J, Fang J, et al. Experimental study on regeneration performance and particle emission characteristics of DPF with different inlet transition sections lengths. *Fuel*. 2020;262: 116487.
55. Bensaid S, Caroca C, Russo N, Fino D. Detailed investigation of non-catalytic DPF regeneration. *Can J Chem Eng*. 2011;89:401-407.
56. Pu X, Cai Y, Shi Y, et al. Diesel particulate filter (DPF) regeneration using non-thermal plasma induced by dielectric barrier discharge. *J Energy Inst*. 2018;91:655-667.
57. Rossomando B, Arsie I, Meloni E, Palma V, Pianese C. Experimental testing of a low temperature regenerating catalytic DPF at the exhaust of a light-duty diesel engine. SAE Technical Paper. 2018.
58. O'Driscoll R, Stettler ME, Molden N, Oxley T, ApSimon HM. Real world CO_2 and NO_x emissions from 149 Euro 5 and 6 diesel, gasoline and hybrid passenger cars. *Sci Total Environ*. 2018;621:282-290.
59. Grigoratos T, Fontaras G, Giechaskiel B, Zacharof N. Real world emissions performance of heavy-duty Euro VI diesel vehicles. *Atmos Environ*. 2019;201:348-359.
60. Gao J, Chen H, Li Y, et al. Fuel consumption and exhaust emissions of diesel vehicles in worldwide harmonized light vehicles test cycles and their sensitivities to eco-driving factors. *Energy Convers Manage*. 2019;196:605-613.

SUPPORTING INFORMATION

Additional supporting information may be found in the online version of the article at the publisher's website.

How to cite this article: Gao J, Chen H, Liu Y, Li Y. Impacts of De-NO_x system layouts of a diesel passenger car on exhaust emission factors and monetary penalty. *Energy Sci Eng*. 2021;9:2268–2280. https://doi.org/10.1002/ese3.1001